Negative Cooperativity Associated with Binding of Multivalent Carbohydrates to Lectins. Thermodynamic Analysis of the "Multivalency Effect"†

Tarun K. Dam,‡ René Roy,§ Daniel Pagé,§ and C. Fred Brewer*,‡

Departments of Molecular Pharmacology and of Microbiology and Immunology, Albert Einstein College of Medicine, Bronx, New York 10461, and Department of Chemistry, Center for Research in Biopharmaceuticals, University of Ottawa, Ottawa, Canada

Received October 4, 2001

ABSTRACT: Our previous study demonstrated that isothermal titration microcalorimetry (ITC) could be used to determine the thermodynamics of binding of a series of synthetic multivalent carbohydrates to the Man/Glc-specific lectins concanavalin A (ConA) and *Dioclea grandiflora* lectin (DGL) [Dam, T. K., Roy, R., Das, S. K., Oscarson, S. and Brewer, C. F. (2000) *J. Biol. Chem. 275*, 14223−14230]. The higher affinities of the multivalent carbohydrates for the two lectins were shown to be due to their greater positive entropy of binding contributions relative to monovalent analogues. In the present study, ITC data from our previous report for binding of di-, tri-, and tetravalent carbohydrate analogues possessing terminal 3,6-di-*O*-(α-D-mannopyranosyl)-α-D-mannopyranoside residues to ConA and DGL were subjected to Hill plot analysis. Hill plots of the binding of monovalent methyl 3,6-di-*O*-(α-D-mannopyranosyl)-α-D-mannopyranoside to ConA and DGL are linear with slopes near 1.0, demonstrating a lack of binding cooperativity and allosteric transitions in the proteins. However, Hill plots for the binding of the di-, tri-, and tetravalent trimannoside analogues to both lectins are curvilinear with decreasing tangent slopes below 1.0, indicating increasing negative cooperativity upon binding of the analogues to the lectins. The curvilinear Hill plots are consistent with decreasing affinity and functional valencies of the multivalent analogues upon sequential binding of lectin molecules to the carbohydrate epitopes of the analogues. The following paper [Dam, T. K., Roy, R., Pagé, D., and Brewer, C. F. (2002) *Biochemistry 41*, 1359−1363] provides direct evidence of the decreasing affinity constants of multivalent carbohydrates upon sequential binding of lectin molecules.

Many naturally occurring carbohydrates and glycoconjugates including glycoproteins and glycolipids are multivalent (cf. ref *1*) and possess increased affinity (avidity) for lectins relative to monovalent analogues (*2*). As a consequence, there has been considerable interest in designing multivalent or "clustered" carbohydrate analogues for high-affinity binding to target lectin receptors (cf. refs *3* and *4*). For example, clustered or "dendritic" GlcNAc-based synthetic analogues with valencies of 2, 4, and 8 on a scaffolding of L-lysine have been reported to possess 5-fold, 25-fold, and 170-fold enhanced affinities, respectively, for wheat germ agglutinin (*5*). Thus, it is important to understand the thermodynamic and mechanistic basis of the enhanced affinities of multivalent glycoconjugates to lectins.

Recently, we reported that isothermal titration microcalorimetry (ITC)[1] could be used to determine the thermodynamics of binding of multivalent carbohydrates to lectins (*6*). The thermodynamics of binding of a series of multivalent carbohydrate analogues of Man to the Man/Glc-specific lectins concanavalin A (ConA) and *Dioclea grandiflora* lectin (DGL) were investigated. The results showed that the value of *n*, the number of binding sites on each lectin monomer, is inversely proportional to the number of binding epitopes (valency) of each carbohydrate. Hence, *n* values close to 1.0, 0.50, and 0.25 for the binding of relatively high- affinity mono-, di-, and tetravalent analogues, respectively, to the two lectins were observed. The enthalpy of binding, ΔH, of the multivalent carbohydrates was observed to be directly proportional to the number of binding epitopes in the higher affinity analogues. For example, ΔH of a tetravalent analogue was nearly 4 times greater than that of the corresponding monovalent analogue. Increases in the K_a values of the two lectins for the multivalent analogues, known as the "multivalency effect", were shown to be due to greater positive entropy ($T\Delta S$) contributions to binding of the multivalent sugars relative to monovalent sugars.

In the present study, ITC data from our previous report (*6*) for the binding of di-, tri-, and tetravalent carbohydrate analogues were subjected to Hill plot analysis, which detects cooperativity in the binding of ligands to macromolecules

† This work was supported by Grant CA-16054 from the National Cancer Institute, Department of Health, Education, and Welfare, and Core Grant P30 CA-13330 from the same agency (C.F.B.). The NMR facility at AECOM was supported by Instrumentation Grants I-S10-RR02309 from the National Institutes of Health and DMB-8413723 from the National Science Foundation.

* To whom correspondence should be addressed [tel, (718) 430-2227; fax, (718) 430-8922; e-mail, brewer@aecom.yu.edu].

‡ Albert Einstein College of Medicine.

§ University of Ottawa.

[1] Abbreviations: ConA, lectin from Jack bean (*Canavalia ensiformis*); DGL, seed lectin from *Diocleia grandiflora*; TriMan, methyl 3,6-di-*O*-(α-D-mannopyranosyl)-α-D-mannopyranoside; ITC, isothermal titration microcalorimetry. All sugars are in the D-configuration.

10.1021/bi015830j CCC: $22.00
Published on Web 12/29/2001

including hemoglobin, various enzymes, and other proteins (cf. refs *7* and *8*). Such plots, for example, have demonstrated positive cooperativity between the subunits of hemoglobin in binding dioxygen. In nearly all examples of binding cooperativity between ligands and macromolecules, the cooperativity has been associated with multisubunit interactions in the protein (cf. ref *9*). Furthermore, there are very few, if any, reports of Hill plot analysis of thermodynamic binding data obtained by ITC, since one of the conditions for Hill plot analysis of ITC data is a lack of subunit interactions in the protein upon ligand binding (*10*). This is because the heat associated with ligand binding cannot be separated from the heat associated with differential protein transitions (*10*). Thus, Hill plot analysis of ITC data is limited to systems in which no allosteric interactions occur in the protein, and binding cooperativity is due to the ligand, as shown below for the binding of multivalent carbohydrates to ConA and DGL, which are both dimeric proteins under the conditions of the measurements (*6*).

The present study demonstrates that ITC data for di-, tri-, and tetravalent carbohydrate analogues binding to ConA and DGL show curvilinear Hill plots with decreasing tangent slopes, while ITC data for binding of the free monovalent trimannoside to both lectins show linear Hill plots with slopes close to 1.0. The negative binding cooperativity of the multivalent analogues to the two lectins is discussed in terms of the mechanisms of enhanced affinities of the multivalent carbohydrates. Hemagglutination inhibition data for binding of the multivalent analogues to the two lectins are also shown to be in agreement with the ITC data.

MATERIALS AND METHODS

DGL was isolated from *D. grandiflora* seeds obtained from Northeastern Brazil (Albano Ferreira Martin Ltd., Sao Paulo, Brazil) as previously described (*11*). The concentration of DGL was determined spectrophotometrically at 280 nm using $A^{1\%,1\ cm} = 12.0$ at pH 5.2 and expressed in terms of monomer ($M_r = 25000$) (*11*). ConA was prepared from Jack bean (*Canavalia ensiformis*) seeds (Sigma Chemical Co.) according to the method of Agrawal and Goldstein (*12*). The concentration of ConA was determined spectrophotometrically at 280 nm using $A^{1\%,1\ cm} = 12.4$ at pH 5.2 (*13*) and expressed in terms of monomer ($M_r = 25600$).

Methyl 3,6-di-*O*-(α-D-mannopyranosyl)-α-D-mannopyranoside (TriMan) was obtained from the Sigma Chemical Co. The synthesis of carbohydrate analogues **1**, **2**, and **3** has also been previously described (*14*). The concentrations of the carbohydrates were determined by modification of the Dubois phenol−sulfuric acid method using appropriate monosaccharides as standards (*15*).

Hemagglutination Inhibition Assay. The assay was performed at 22 °C using a 2-fold serial dilution technique (*16*) and 3% (v/v) rabbit erythrocytes in Hepes buffer (0.1 M Hepes, 0.15 M NaCl, 1 mM $CaCl_2$, and 1 mM $MnCl_2$, pH 7.2). The minimum concentration of saccharide required for complete inhibition of four hemagglutination doses was determined.

Isothermal Titration Microcalorimetry. ITC experiments were performed using a model MCS instrument from Microcal, Inc. (Northampton, MA). Injections of 4 μL of carbohydrate solution were added from a computer-controlled 250 or 100 μL microsyringe at an interval of 4 min into the sample solution of lectin (cell volume = 1.3424 mL) with stirring at 350 rpm. Control experiments performed by making identical injections of saccharide into a cell containing buffer without protein showed insignificant heats of dilution. The concentrations of lectins were 0.015−0.14 mM and those of the sugars were 0.16−4.0 mM, respectively. Titrations were done at pH 5.0−5.2 and at NaCl concentrations from 0 to 0.15 M where the lectin−carbohydrate complexes were soluble. The experimental data were fitted to a theoretical titration curve using software supplied by Microcal, with ΔH (enthalpy change in kcal/mol), K_a (association constant in M^{-1}), and n (number of binding sites per monomer) as adjustable parameters. The quantity $c = K_a M_t(0)$, where $M_t(0)$ is the initial macromolecule concentration, is of importance in titration microcalorimetry (*17*). All experiments were performed with c values in the range of $1 < c < 200$. The instrument was calibrated using the calibration kit containing ribonuclease A (RNase A) and cytidine 2′-monophosphate (2′-CMP) supplied by the manufacturer. Thermodynamic parameters were calculated from the equation

$$\Delta G = \Delta H - T\Delta S = -RT \ln K_a$$

where ΔG, ΔH, and ΔS are the changes in free energy, enthalpy, and entropy of binding. T is the absolute temperature, and $R = 1.98$ cal mol^{-1} K^{-1}.

Scatchard and Hill Plot ITC Data Analysis. The total concentration of ligand $X_t(i)$ as well as lectin $M_t(i)$ after the ith injection and the heat evolved on the ith injection $Q(i)$ are readily available from the ITC raw data file after each experiment. The concentration correction is automatically done by the Origin software.

The concentration of bound ligand X_b(i) after the ith injection is

$$X_b(i) = [Q(i)/(\Delta H V_o)] + X_b(i-1) \qquad (1)$$

where $Q(i)$ (μcal) is the heat evolved on ith injection, ΔH (cal mol^{-1}) is the enthalpy change, V_o (mL) is the active cell volume, and X_b (mM) is the concentration of bound ligand. X_b is equal to M_b, the concentration of bound protein, and in the present study of multivalent ligands, the more general expression is $M_b = (X_b)$(functional valency of ligand). The concentration of free ligand (X_f) after the ith injection was determined as

$$X_f(i) = X_t(i) - X_b(i) \qquad (2)$$

For Scatchard analysis, $r(i)$ was plotted against $r(i)/X_f(i)$, where $r(i)$ is $[X_b(i)]$(functional valency of ligand)/$M_t(i)$, and Hill plots were constructed by plotting $\log[Y(i)/[1 - Y(i)]]$ versus $\log[X_f(i)]$, where $Y(i)$ is $[X_b(i)]$(functional valency of ligand)/$M_t(i)$, which are modified versions of the Scatchard and Hill plots (cf. ref *8*) that take into account the functional valency of the ligand. The functional valencies of **1**, **2**, and **3** binding to ConA and DGL were obtained from our previous study (*6*) and are listed in the figure legends for the respective Scatchard and Hill plots.

A program was created using Microsoft Excel for construction of Scatchard and Hill plots. Work sheet data of total ligand as well as total lectin concentration and the

amount of heat evolved were copied from the ITC raw data file and pasted on the appropriate columns of the program. After calculation the program shows the profiles of Hill and Scatchard plots. Delta Graph was then used for further analysis of the plots.

The validity of the information obtained from the Hill plot [$\log[Y/(1 - Y)]$ versus $\log(X_f)$] was tested by directly fitting the binding data of monovalent trimannoside to the Hill equation. The Hill slope was found to be the same by direct fitting or plotting the Hill equation data. Similar attempts at direct fitting of the ITC data for the multivalent analogues failed since the Hill *n* values change throughout the binding process.

RESULTS AND DISCUSSION

Our previous ITC study (*6*) concluded that the greater K_a values of multivalent carbohydrate analogues **1**−**3**, relative to Triman, for ConA and DGL were due to their relatively positive binding entropies ($T\Delta S$). In terms of a physical model for the enhanced affinities of the multivalent carbohydrates (*6*), clustering of binding epitopes was concluded to result in an increase in the macroscopic affinity constants of the analogues due to increases in the microscopic equilibrium constants associated with the respective epitopes. In the present study, Hill plots of the ITC data for binding of multivalent analogues **1**−**3** to ConA and DGL are shown to be curvilinear with decreasing tangent slope values of less than 1.0. The results are discussed in terms of the mechanisms of enhanced affinities of the multivalent carbohydrates.

ITC Data. Previous ITC studies have shown that TriMan is a monovalent ligand for ConA (*18*) and DGL (*19*). Synthetic analogues **1**, **2**, and **3** in Figure 1 possess two, three, and four trimannoside moieties, respectively, and, hence, are nominally di-, tri-, and tetravalent for binding to ConA and DGL. Previous ITC data for the binding of TriMan, **1**, **2**, and **3** to ConA and DGL are given in Tables 1 and 2, respectively (*6*). Triman possesses ∼40-fold higher affinity than MeaMan for ConA (*18*) and nearly 250-fold higher affinity for DGL relative to the monosaccharide (*19*). These differences are due to the extended binding sites of ConA and DGL for the trimannoside as revealed by their respective X-ray crystal complexes with the trisaccharide (*20*, *21*). Hence, analogues **1**−**3** incorporate multiple high-affinity binding epitopes for both lectins.

Multivalent analogues **1**−**3** all show enhanced affinities for ConA (Table 1) and DGL (Table 2) relative to TriMan. Analogue **1** shows a 6-fold greater K_a value for ConA and a 5-fold greater K_a value of DGL. Analogues **2** and **3** show 11- and 35-fold higher K_a values for ConA, respectively, and 8- and 53-fold higher K_a values for DGL relative to the trimannoside. Thus, analogue **3** exhibits substantially higher affinities for ConA and DGL relative to TriMan. These findings are in agreement with hemagglutination inhibition data in Table 3.

The *n* values for **1** binding to ConA and DGL are 0.53 (Table 1) and 0.51 (Table 2), respectively, which are close to the theoretical value of 0.50 for binding of a divalent ligand to the lectins (*6*). Hence, **1** is functionally bivalent for ConA and DGL. The *n* values for **3** binding to ConA and DGL are 0.26 and 0.25, respectively, which are very close to the theoretical value of 0.25 for a tetravalent ligand binding to the lectins. This indicates that all four trimannoside moieties of **3** bind to ConA and DGL. The fact that both lectins precipitate with **3** after the ITC experiments indicates that each molecule of **3** cross-links four lectin molecules, respectively, and forms a two- or three-dimensional cross-linked complex which is required for precipitation of the complex (*22*).

The value of *n* for the binding of **2** to ConA is 0.51 instead of the predicted value of 0.33, based on the structural valency of the triantennary analogue (*6*). Hence, **2** is functionally bivalent in binding to ConA. However, the *n* value for **2** binding to DGL is 0.40, which is still higher than 0.33 for trivalent binding. This suggests that ∼60% of **2** is involved in trivalent binding to DGL, and ∼40% of **2** is involved in bivalent binding to the lectin.

Analogue **1** has a ΔH value of −26.2 kcal/mol for binding to ConA, which is nearly twice the ΔH value of −14.7 kcal/mol for TriMan (Table 1). The same is true for **1** binding to DGL (Table 2). The ΔH value for tetravalent analogue **3** binding to ConA is −53.0 kcal/mol, which is approximately 4 times as great as the ΔH value of the free trimannoside (−14.7 kcal/mol). The ΔH value for **3** binding to DGL is −58.7 kcal/mol, which is also nearly 4 times as great as the ΔH value of the free trimannoside (−16.2 kcal/mol). The ΔH values of analogue **2** are more complicated since the analogue appears to be close to bivalent for ConA ($n = 0.51$) and partially trivalent for DGL ($n = 0.40$). These results indicate that the ΔH values of relatively high-affinity multivalent carbohydrates binding to ConA and DGL are approximately the sum of the ΔH values of the individual binding epitopes in the analogues (*6*).

*Thermodynamic Basis for the Enhanced Affinities of Analogues **1**−**3***. The increased affinities of analogues **1**−**3** for ConA and DGL are associated with their epitopes binding to separate lectin molecules (*6*). As an example, the observed K_a value for **3** is an average of the four microscopic K_a values at each of its four epitopes, since each of the four epitopes is involved in binding to a separate lectin molecule. It follows that if ΔH is constant at each epitope and is approximately the same as that of TriMan (Tables 1 and 2) (*6*), then increases in the overall microscopic K_a values of the four epitopes require more favorable $T\Delta S$ contributions than that of TriMan. An estimate of the overall favorable $T\Delta S$ contribution to the enhanced affinity of **3** relative to Triman was previously given as the differences in ΔG values between **3** and Triman, which are 2.1 and 2.3 kcal/mol for ConA and DGL, respectively.

The fact that analogues **1**−**3** must have microscopic K_a values associated with their multiple epitopes leads to a prediction regarding their binding interactions with lectins such as ConA and DGL. Sequential binding of each epitope in analogues **1**−**3** results in diminished valency for each molecule; therefore, binding of the analogues should occur with negative cooperativity as their effective valency decreases. This expected decrease in functional valency of the multivalent analogues and concomitant negative binding cooperativity can be tested with Scatchard and Hill plots of the ITC data for each analogue.

*Hill Plots of the ITC Data for the Binding of Multivalent Analogues **1**−**3***. The Hill plot, in which log [free ligand] is plotted versus log(fraction of bound protein)/(fraction of free protein), has been used to investigate cooperativity in a

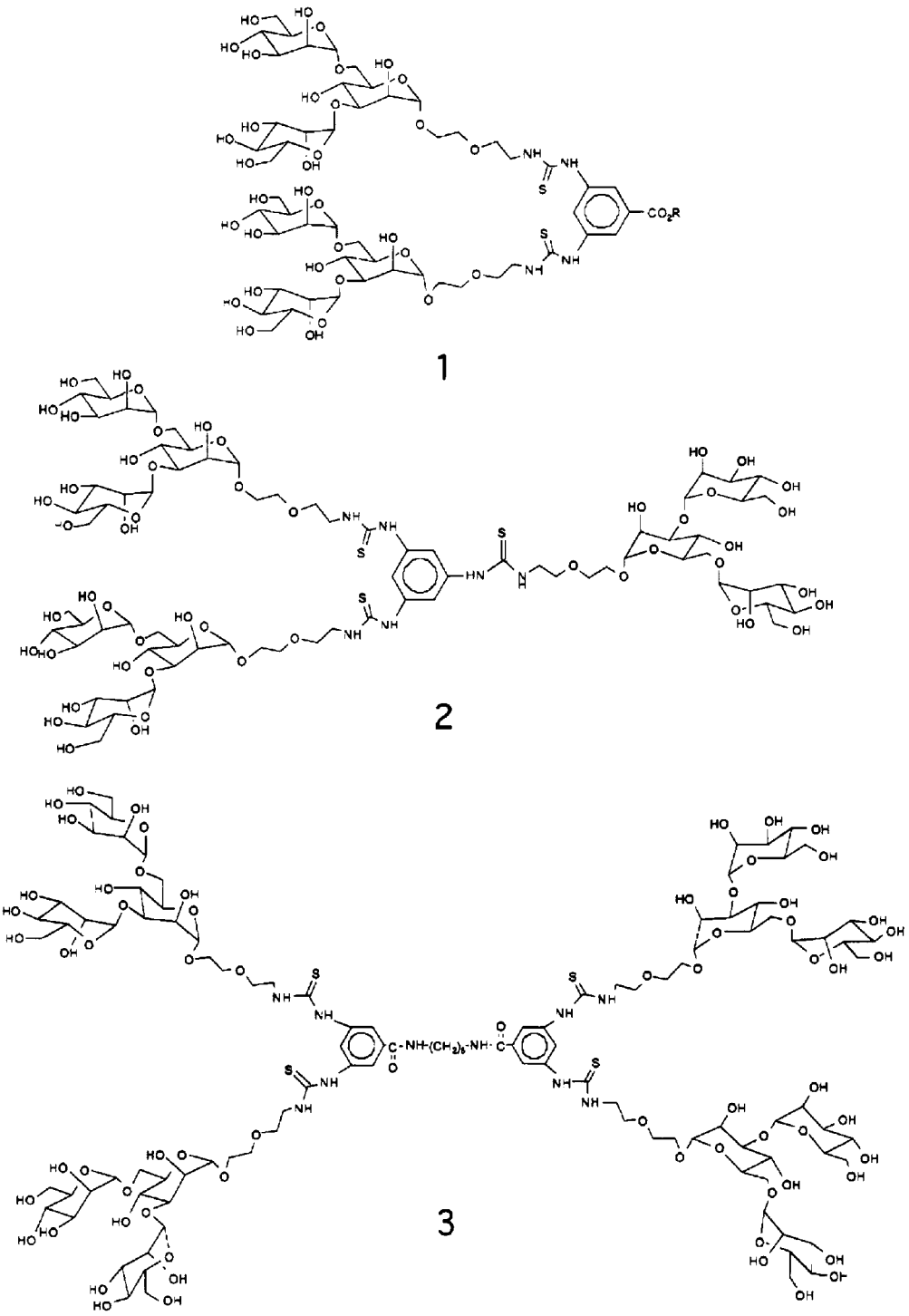

FIGURE 1: Structures of multivalent carbohydrate analogues **1**, **2**, and **3**.

variety of ligand−protein systems (cf. refs *7* and *8*). Such plots may typically show evidence for positive or negative cooperativity in the binding of monovalent ligands to multisubunit proteins. Ligand binding without cooperativity gives rise to a linear Hill plot with a slope of 1.0. Ligand binding with positive cooperativity gives rise to Hill plots with slopes greater than 1.0, while ligand binding with negative cooperativity gives Hill plots with slopes less than 1.0. Thus, the Hill plot has the advantage of assigning numerical values to the degree of cooperativity of the system, as compared to the Scatchard plot (*23*), which is often used to investigate binding cooperativity as well other binding parameters. The Hill plot also has the advantage of being a logarithmic representation which allows plotting of all theoretically obtainable data, unlike double-reciprocal or half-reciprocal plots that often have open upper limits on the abscissa and ordinate (*24*). Hill plots can also reveal cooperativity associated with binding of multivalent ligands to noncooperative multisubunit proteins such as ConA and DGL, as demonstrated below. In using Hill plot analysis of the binding of a multivalent ligand such as the sugars in the present study, the term for the fraction of bound ligand, X_b/M_t, is corrected for the valency of the sugar to give (X_b)(functional valency of sugar)$/M_t$, which is a modification of the classical Hill plot as well as the Scatchard plot (see Materials and Methods).

Table 1: ITC-Derived Thermodynamic Binding Parameters for Concanavalin A with TriMan and Multivalent Sugar Analogues **1**−**3** at 27 °C (from Ref 6)

	K_a[a] ($M^{-1} \times 10^{-4}$)	$-\Delta G$[b] (kcal/mol)	$-\Delta H$[c] (kcal/mol)	$-T\Delta S$[d] (kcal/mol)	n[e] (no. of sites/monomer)
TriMan[f]	39	7.6	14.7	7.1	1.0
1	250	8.7	26.2	17.5	0.53
2	420	9.0	29.0	20.0	0.51
3	1350	9.7	53.0	43.3	0.26

[a] Errors in K_a range from 1% to 7%. [b] Errors in ΔG are less than 1%. [c] Errors in ΔH are 1−4%. [d] Errors in $T\Delta S$ are 1−7%. [e] Errors in n are less than 2%. [f] Methyl 3,6-di-*O*-(α-D-mannopyranosyl)-α-D-mannopyranoside.

Table 2: ITC-Derived Thermodynamic Binding Parameters for *D. grandiflora* Lectin with TriMan and Multivalent Sugar Analogues **1**−**3** at 27 °C (from Ref *6*)

	K_a[a] ($M^{-1} \times 10^{-4}$)	$-\Delta G$[b] (kcal/mol)	$-\Delta H$[c] (kcal/mol)	$-T\Delta S$[d] (kcal/mol)	n[e] (no. of sites/monomer)
TriMan[f]	122	8.3	16.2	7.9	1.0
1	590	9.2	27.5	18.3	0.51
2	1000	9.6	32.2	22.6	0.40
3	6500	10.6	58.7	48.1	0.25

[a] Errors in K_a range from 1% to 7%. [b] Errors in ΔG are less than 1%. [c] Errors in ΔH are 1−4%. [d] Errors in $T\Delta S$ are 1−7%. [e] Errors in n are less than 2%. [f] Methyl 3,6-di-*O*-(α-D-mannopyranosyl)-α-D-mannopyranoside.

Table 3: Comparison of K_a Values Derived from Isothermal Titration Microcalorimetry Measurements[a] with Hemagglutination Inhibition Measurements for ConA and DGL Binding to Multivalent Analogues **1**−**3**

	K_a ($M^{-1} \times 10^{-4}$)[a,b]	minimum inhibitory concn (μM)[b]
	Con A	
TriMan	39 (1)	29 (1)
1	250 (6)	5.0 (6)
2	420 (11)	2.6 (11)
3	1350 (34)	1.0 (29)
	DGL	
TriMan	122 (1)	7 (1)
1	590 (4)	1.3 (5)
2	1000 (8)	0.97 (7)
3	6500 (53)	0.11 (63)

[a] From ref *6*. [b] Relative values are in parentheses.

The Hill plot of ITC data for TriMan binding to ConA is shown in Figure 2. The plot is essentially a straight line with a slope of 0.94, which is close to a value of 1.0 for noncooperative binding interactions (*7*, *8*). A similar plot with a slope of 0.95 is observed for DGL (not shown). Linear Hill plots are observed for TriMan concentrations up to 1 mM. Above this concentration of TriMan, the Hill plots exhibit some curvature, due to possible sugar−sugar interactions of the free TriMan. Hence, below 1 mM monovalent TriMan binds without cooperativity effects, as has been inferred from an ITC-derived Scatchard plot (*18*), which is linear and which was confirmed in the present study (Figure 3). Linear Scatchard plots for the binding of monosaccharides to ConA have been previously reported (*25*).

Importantly, the absence of allosteric interactions in ConA and DGL upon binding TriMan allows application of Hill plot analysis to the ITC binding data for analogues **1**−**3** since

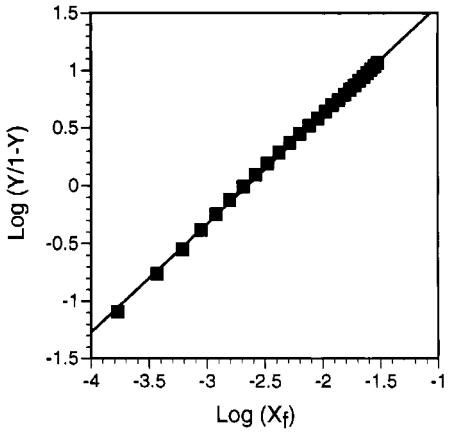

FIGURE 2: Hill plot of the ITC data of TriMan (800 μM) binding to ConA (20 μM). In the plot, $Y = (X_b)$(functional valency of sugar)/M_t, where X_b is the concentration of bound ligand, M_t is the concentration of total lectin, and X_f is the concentration of free sugar. The functional valency of TriMan is 1, as determined previously (*6*).

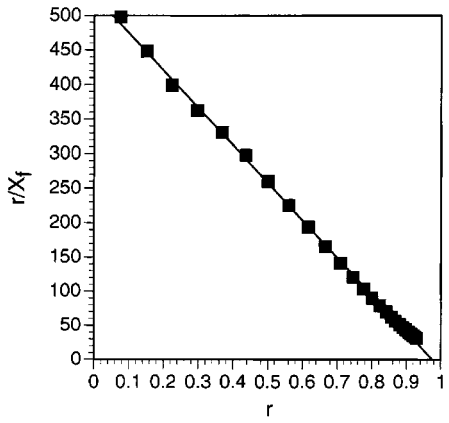

FIGURE 3: Scatchard plot of the ITC data for TriMan (800 μM) binding to ConA (20 mM). In the plot, $r = (X_b)$(functional valency of sugar)/M_t, where X_b is the concentration of bound ligand, M_t is the concentration of total lectin, and X_f is the concentration of free ligand.

the incremental heats measured upon sugar addition and binding are proportional to the number of moles of ligand bound and not due to allosteric transitions in the lectins. These general conditions are required for Hill plot analysis of ITC data (*10*). In addition, all of the ITC binding data for multivalent sugars **1**−**3** and TriMan were obtained at sugar concentrations well below 1 mM to avoid possible sugar−sugar interactions. The concentration dependence of the binding of the multivalent sugars to the two lectins is also consistent with sugar−protein interactions and not sugar−sugar interactions (data to be shown elsewhere).

Scatchard plots of the ITC data for analogues **1**−**3** binding to ConA and DGL are curvilinear, as shown for analogue **3** binding to ConA (Figure 4). The concave nature of the Scatchard plots as seen in Figure 4 suggests that analogues **1**−**3** bind to both lectins with negative cooperativity. Therefore, Hill plots of the ITC binding data for **1**−**3** to both lectins were examined.

Hill plots of the ITC data for analogues **1**−**3** binding to ConA are shown in Figure 5. All three plots are curvilinear rather than linear. The plots are also disposed around the zero point on the ordinate, as observed for monovalent TriMan (Figure 2), after correction for the functional

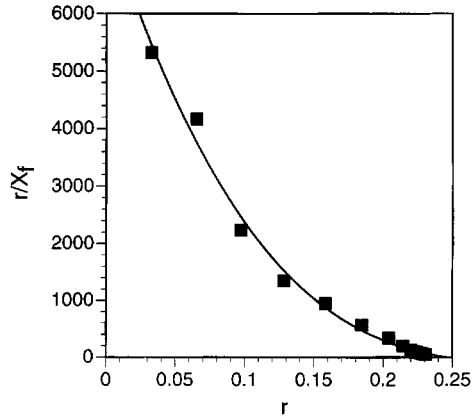

FIGURE 4: Scatchard plot of the ITC data of analogue **3** (240 μM) binding to ConA (20 μM). The definitions of r and X_f are given in the legend of Figure 3. The functional valency of **3** is 4 for ConA (*6*).

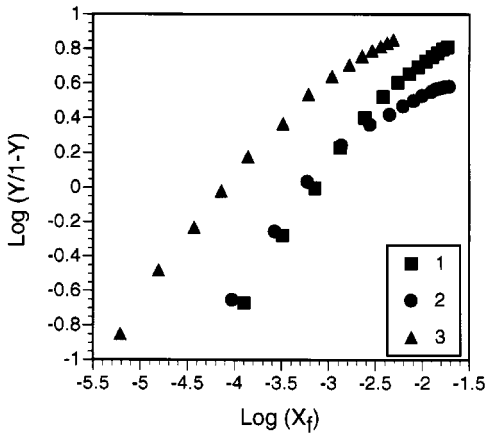

FIGURE 5: Hill plots of the ITC data for analogues **1**−**3** binding to ConA (20 μM). The concentration of **1** was 650 μM, **2** was 670 μM, and **3** was 240 μM. The definition of Y is given in the legend of Figure 2. The functional valencies of **1** and **2** are 2, and the functional valency of **3** is 4, as determined previously (*6*).

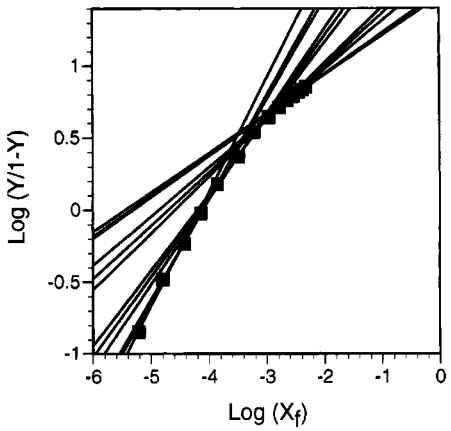

FIGURE 6: Tangent slopes of progressive three-point intervals of the Hill plot for analogue **3** with ConA.

valencies of the multivalent sugars. This provides confirmation of the ITC-derived functional valencies of **1**, **2**, and **3** for ConA in our previous study (*6*). The tangent slopes of progressive three-point intervals of the *x*-axis of the Hill plot for **3** are shown in Figure 6, which shows decreasing tangent slopes along the binding curve. Figure 7 shows a bar graph comparison of the three-point tangent slopes of all three analogues binding to ConA. All three analogues possess

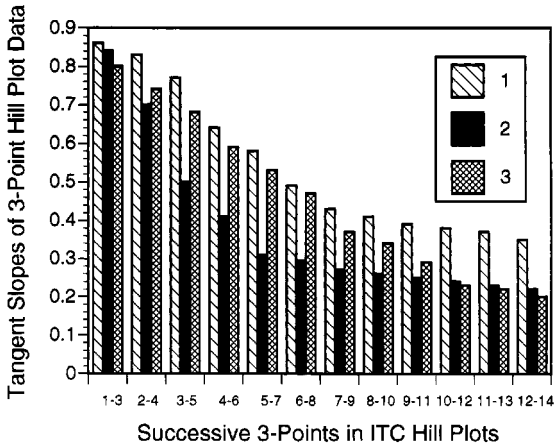

FIGURE 7: Bar graphs of the three-point tangent slopes of the ITC data Hill plots of analogues **1**−**3** binding to ConA.

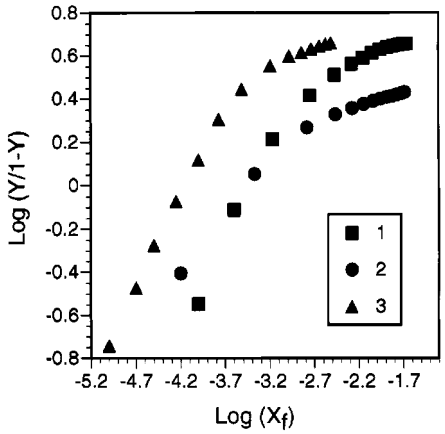

FIGURE 8: Hill plots of the ITC data for analogues **1**−**3** binding to DGL (15−17 μM). The concentration of **1** was 670 μM, **2** was 690 μM, and **3** was 160 μM. The functional valencies for **1**, **2**, and **3** used in the Hill plots were 2, 2.5, and 4, respectively, as determined previously (*6*).

initial tangent slope values between 0.8 and 0.9. The final tangent slope value of **1** is 0.35 while the final values for **2** and **3** are 0.24 and 0.22, respectively. These results indicate increasing negative cooperativity in the binding of ConA to analogues **1**−**3**, with greater negative binding cooperativity for **2** and **3** relative to **1**.

The Hill plots for **1**−**3** binding to DGL are also curvilinear, as shown in Figure 8. The plots are also disposed around the zero point on the ordinate, as observed for monovalent TriMan (not shown), after correction for the functional valencies of the multivalent sugars. This also provides confirmation of the ITC-derived functional valencies of **1**, **2**, and **3** for DGL in our previous study (*6*). The bar graphs of the three-point tangent slopes of the analogues are shown in Figure 9. The initial tangent slope values for **1** and **3** are close to 0.90, and that for **2** is 0.65. The final tangent slopes for all three multivalent carbohydrates are close to 0.1. These results indicate increasing negative cooperativity in the binding of DGL to analogues **1**−**3**. However, the tangent slopes of the curvilinear Hill plots for ConA and DGL with **1**−**3** are distinct for the two lectins. All three analogues possess lower final tangent slope values in binding to DGL relative to ConA, indicating greater increasing negative cooperativity in binding the last fraction of DGL molecules relative to ConA. Differences in the fine carbohydrate

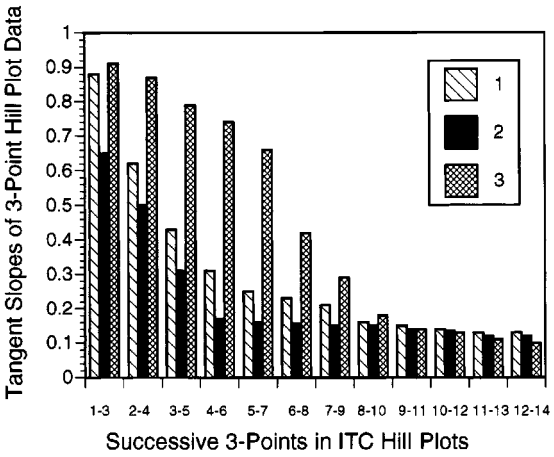

FIGURE 9: Bar graphs of the three-point tangent slopes of the ITC data Hill plots for analogues **1**−**3** binding to DGL.

Scheme 1

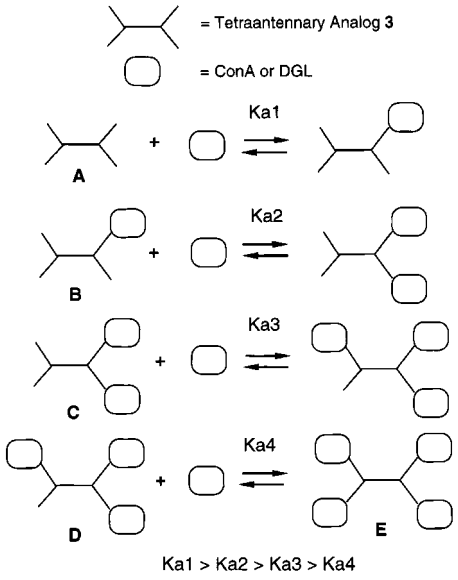

binding specificities of the two lectins have been previously reported (*6*, *26*), as well as small differences in the structures of the two lectins (*21*). Importantly, the increasing negative binding cooperativity of ConA and DGL observed in Figures 7 and 9 is due to the multivalency of **1**−**3** and not the lectins since TriMan shows no cooperativity effects.

The physical basis for the increasing negative binding cooperativity of **1**−**3** can be understood, in part, by the reduction in functional valency of the analogues as they bind an increasing number of lectin molecules. For example, Scheme 1 shows the various microequilibria constants for **3** as it sequentially binds one, two, three, and four molecules of ConA (or DGL). The functional valency of unbound **3** (species A) is tetravalent, the functional valency of **3** with one bound lectin molecule (species B) is trivalent, the functional valency of **3** with two bound lectin molecules (species C) is divalent, and the functional valency of **3** with three bound lectin molecules (species D) is monovalent. The increasingly curvilinear Hill plots in Figures 5 and 8 for **3** binding to ConA and DGL, respectively, are consistent with the decreasing valency and increasing negative binding cooperativity of **3** with increasing sequential occupancy of the four epitopes of the analogue. The same is true for analogues **1** and **2** with ConA and DGL in Figures 5 and 8, respectively.

Another physical factor which may play a role in the curvilinear Hill plots of **1**−**3** with ConA and DGL is the formation of noncovalent cross-linked complexes between lectin molecules and multivalent carbohydrates (*6*). Scheme 1 is overly simplified in that each lectin molecule, represented as a monomer in the scheme, is actually a dimer under the conditions of the experiment (pH 5.2 and low ionic strength). Hence, each lectin molecule (ConA or DGL) is capable of binding and cross-linking the multivalent carbohydrates in the present study. Analogues **1** and **2** are divalent for ConA (Table 1) and may form linear cross-linked complexes with the protein. Analogue **3** is tetravalent for ConA (Table 1) and also expected to form noncovalent cross-linked complexes with the lectin. The fact that **3** precipitates with ConA approximately 1 h after mixing supports this conclusion (*6*). Analogue **2** is partially trivalent for DGL (Table 2), while **3** is tetravalent for DGL. Hence, it is possible that the formation of cross-linked lattices with analogues **1**−**3** may affect their binding interactions with successive lectin molecules, which contributes to the increasing negative cooperativity observed in their Hill plots with both lectins. Preliminary evidence indicates that such cross-linking interactions along with the decreasing functional valencies of **1**−**3** upon binding sequential lectin molecules play a role in the curvilinear Hill plots of the analogues (details to be presented elsewhere).

Microscopic K_a Values and Kinetic Effects of Multivalency. The observed K_a values for multivalent analogues **1**−**3** in Tables 1 and 2 are the average of the microscopic binding free energy terms ($-\Delta G$) of the different epitopes of the analogues. For example, analogue **3** possesses four trimannoside binding epitopes, and ITC data in Tables 1 and 2 indicate that all four arms of **3** are involved in binding to separate molecules of ConA and DGL, respectively. As shown in Scheme 1, the four microequilibrium constants of **3** can be represented by K_{a1}, K_{a2}, K_{a3}, and K_{a4} for binding of a ConA or DGL molecule to the first arm of **3** (species **A**), to the second arm of **3** (species **B**), etc. Hence, the observed ΔG values of **3** (ΔG_{obs}) for ConA and DGL in Tables 1 and 2 are the average of the four microscopic ΔG terms, or $\Delta G_{obs}(\mathbf{3}) = (\Delta G_1 + \Delta G_2 + \Delta G_3 + \Delta G_4)/4$. The relative values of ΔG_1, ΔG_2, ΔG_3, and ΔG_4 must decrease, based on the decreasing ΔG values (Tables 1 and 2) of **2**, **1**, and TriMan, respectively, which have the same valencies as species **B**, **C**, and **D** of **3**, respectively. Thus, it is expected that $K_{a1} > K_{a2} > K_{a3} > K_{a4}$ for **3** binding to ConA and DGL, as shown in Scheme 1.

The following paper in this series (*29*) provides direct experimental evidence for the decreasing microscopic K_a values of **1** and **2** in binding ConA molecules to their different epitopes (*29*).

Hemagglutination Inhibition Data. Hemagglutination inhibition data for Triman and **1**−**3** with ConA and DGL are shown in Table 3. The relative inhibition potencies of the carbohydrates are shown to be similar to their respective K_a values in Tables 1 and 2. These results indicate that both hemagglutination inhibition and ITC measurements monitor the same thermodynamic binding equilibrium of the carbohydrates to the lectins. Similar comparisons of hemagglutination inhibition and ITC data with other sugars and both lectins have lead to the same conclusions (cf. refs *26* and *27*).

These findings are in contrast to recent results by Toone and co-workers (*28*). These workers reported that hemagglutination inhibition and ITC measurements reflect different relative binding affinities of multivalent carbohydrates to ConA. Multivalent analogues containing up to six Man residues were synthesized and were shown to have enhanced affinities, relative to MeαMan, for ConA by hemagglutination inhibition measurements, but not enhanced K_a values by ITC measurements. They concluded that the hemagglutination inhibition measurements did not reflect the true thermodynamic binding affinities of the multivalent sugars to ConA since the ITC data indicated no enhanced affinities of the same sugars. However, the scaffoldings used to construct the multivalent Man molecules used in their study possess an increasing number of benzene rings with an increasing number of Man residues in the analogues. It is quite possible that the tetrameric and hexameric analogues with the greatest number of benzene rings (four in the hexamer case) may have stacked together in the aqueous buffer at the higher concentrations required for the ITC measurements (∼25 mM). These stacking interactions could interfere with the enhanced affinities of the carbohydrate analogues under ITC conditions, as compared to the conditions of their hemagglutination inhibition experiments which required much lower sugar concentrations (<50 μM). Hence, the difference in hemagglutination inhibition and ITC data for the higher valency sugar analogues reported by Dimick et al. (*28*) may be due to scaffolding effects of the analogues, and not to intrinsic affinity differences of the two methods.

Another important difference in the Dimick et al. (*28*) study is their use of epitope equivalents for the concentrations of the multivalent carbohydrate analogues rather than molar concentrations of the sugars. Their hemagglutination and ITC data are both divided by the total number of Man residues in their respective analogues. The authors stated that this was done with the assumption that no cooperativity between Man residues occurs in the binding processes. However, there is strong negative cooperativity in the binding of multivalent analogues such as those in Tables 1 and 2 in the present study. Hence, the condition of no cooperativity between binding residues in multivalent carbohydrates to lectins may not be true. Another problem is that the actual number of sugar residues in a multivalent carbohydrate that bind to a lectin is an experimental parameter, not a structural parameter. This was demonstrated in our recent study of analogue **2** (Figure 2), which is structurally trivalent, but ITC data demonstrate that it has a functional valency of 2 for ConA and a functional valency between 2 and 3 for DGL (*6*). Hence, assigning the concentration of a multivalent sugar on the basis of the number of sugar residues in the molecule is incorrect. Furthermore, the units for all thermodynamic binding assays is molar, not equivalent concentrations.

It is important to note that the concentration of protein in the present study is given in terms of monomer concentration since there is no binding cooperativity between subunits of ConA or DGL. Each monomer of the lectin can thus be treated as a separate binding entity.

REFERENCES

1. Varki, A., Cummings, R., Esko, J., Freeze, H., Hart, G., and Marth, J. (1999) *Essentials of Glycobiology*, Cold Spring Harbor Laboratory Press, Cold Spring Harbor, NY.
2. Lee, Y. C. (1993) *FASEB J. 6*, 3193−3200.
3. Roy, R. (1996) *Curr. Opin. Struct. Biol. 6*, 692−702.
4. Kiessling, L. L., and Pohl, N. (1996) *Chem. Biol. 3*, 71−77.
5. Zanini, D., and Roy, R. (1997) *Bioconjugate Chem. 8*, 187−192.
6. Dam, T. K., Roy, R., Das, S. K., Oscarson, S., and Brewer, C. F. (2000) *J. Biol. Chem. 275*, 14223−14230.
7. Stryer, L. (1988) *Biochemistry*, 3rd ed., W. H. Freeman and Co., New York.
8. Di Cera, E. (1995) *Thermodynamic Theory of Site-Specific Binding Processes in Biological Macromolecules*, Cambridge University Press, New York.
9. Perutz, M. F. (1989) *Qt. Rev. Biophys. 22*, 139−236.
10. Indyk, L., and Fisher, H. F. (1998) *Methods Enzymol. 295*, 350−364.
11. Moreira, R. A., Barros, A. C. H., Stewart, J. C., and Pusztai, A. (1983) *Planta 158*, 63−69.
12. Agrawal, B. B. L., and Goldstein, I. J. (1967) *Biochim. Biophys. Acta 147*, 262−271.
13. Goldstein, I. J., and Poretz, R. D. (1986) in *The Lectins* (Liener, I. E., Sharon, N., and Goldstein, I. J., Eds.) pp 35−244, Academic Press, New York.
14. Roy, R., Page, D., Perez, S. F., and Bencomo, V. V. (1998) *Glycoconjugate J. 15*, 251−263.
15. Saha, S. K., and Brewer, C. F. (1994) *Carbohydr. Res. 254*, 157−167.
16. Osawa, T., and Matsumoto, I. (1972) *Methods Enzymol. 28B*, 323−327.
17. Wiseman, T., Williston, S., Brandt, J. F., and Lin, L.-N. (1989) *Anal. Biochem. 179*, 131−137.
18. Mandal, D. K., Kishore, N., and Brewer, C. F. (1994) *Biochemistry 33*, 1149−1156.
19. Dam, T. K., Oscarson, S., and Brewer, C. F. (1998) *J. Biol. Chem. 273*, 32812−32817.
20. Naismith, J. H., and Field, R. A. (1996) *J. Biol. Chem. 271*, 972−976.
21. Rozwarski, D. A., Swami, B. M., Brewer, C. F., and Sacchettini, J. C. (1998) *J. Biol. Chem. 273*, 32818−32825.
22. Brewer, C. F. (1996) *Chemtracts: Biochem. Mol. Biol. 6*, 165−179.
23. Scatchard, G. (1949) *Ann. N.Y. Acad. Sci. 51*, 660−672.
24. Weber, G., and Anderson, S. (1965) *Biochemistry 4*, 1942−1947.
25. So, L. L., and Goldstein, I. J. (1968) *Biochim. Biophys. Acta 165*, 398−404.
26. Dam, T. K., Cavada, B. S., Grangeiro, T. B., Santos, C. F., de Sousa, F. A. M., Oscarson, S., and Brewer, C. F. (1998) *J. Biol. Chem. 273*, 12082−12088.
27. Gupta, D., Oscarson, S., Raju, T. S., Stanley, P., Toone, E. J., and Brewer, C. F. (1996) *Eur. J. Biochem. 242*, 320−326.
28. Dimick, S. M., Powell, S. C., McMahon, S. A., Moothoo, D. N., Naismith, J. H., and Toone, E. J. (1999) *J. Am. Chem. Soc. 121*, 10286−10296.
29. Dam, T. K., Roy, R., Pagé, D., and Brewer, C. F. (2002) *Biochemistry 41*, 1359−1363.

BI015830J